NATIONAL ADVISORY COMMITTEE FOR AERONAUTICS

TECHNICAL NOTE 4107

EFFECTS OF AIRPLANE FLEXIBILITY ON WING STRAINS IN ROUGH AIR AT 5,000 FEET AS DETERMINED BY FLIGHT TESTS OF A LARGE SWEPT-WING AIRPLANE

By Richard H. Rhyne and Harold N. Murrow

Langley Aeronautical Laboratory
Langley Field, Va.

Washington
September 1957

NATIONAL ADVISORY COMMITTEE FOR AERONAUTIC

TECHNICAL NOTE 4107

EFFECTS OF AIRPLANE FLEXIBILITY ON WING STRAINS IN ROUGH AIR AT 5,000 FEET AS DETERMINED BY FLIGHT TESTS OF A LARGE SWEPT-WING AIRPLANE

By Richard H. Rhyne and Harold N. Murrow

SUMMARY

A flight investigation has been made on a large swept-wing bomber airplane in rough air at 5,000 feet to determine the effects of wing flexibility on wing bending and shear strains. In order to evaluate the overall magnitude of the aeroelastic effects on the strains and their variation with spanwise location, amplification factors defining the ratio of the strains in rough air to the strains expected for a "rigid" and "quasi-rigid" airplane were determined. The results obtained indicate that the aeroelastic effects are rather large, particularly at the outboard stations. The effects of dynamic aeroelasticity appear to increase the strains from 0 to 170 percent depending upon the spanwise station. On the other hand, the relieving effects of static aeroelasticity appear to reduce the strain amplification in rough air by a significant amount.

INTRODUCTION

The stresses that develop in aircraft structures in flight through turbulent air are, in many cases, strongly influenced by aeroelastic effects. In the study of these aeroelastic effects, flight-test studies have been made on several unswept-wing airplanes that have been classified from "rather stiff" to "rather flexible" (refs. 1 to 4). Analytical methods have also been developed in references 5 to 7 for calculating the structural response of unswept-wing airplanes to atmospheric turbulence. The results obtained in such calculations show good correlation with the results of flight-test studies for the unswept-wing airplanes so far considered.

The response of swept-wing airplanes in rough air involves a number of complications not present in the case of unswept-wing airplanes. These complications are due principally to the increased importance of torsion for swept-wing airplanes. This torsion in turn results in significant effects on both the airplane aerodynamics and stability. In addition, the

airplane vibratory modes may no longer be approximated by simple beam-bending theory but may require consideration of coupled bending-torsion modes. Few experimental data exist on the character and magnitude of these problems.

In view of the lack of experimental data on the many questions involved in the behavior of a swept-wing airplane in rough air, a flight investigation on a flexible swept-wing airplane was undertaken. The general aim of this investigation was to determine the magnitude of the aeroelastic effects on the wing strains and the importance of the many factors involved in the gust response. These results would then serve to indicate the elements necessary for a successful dynamic analysis and also serve to provide test data which would be useful for correlation with theory.

The present paper describes the flight-test conditions and presents the results obtained from the initial evaluations of the wing strain measurements. The results presented are principally limited to the establishment of the overall character and magnitude of the dynamic flexibility or vibratory effects on the wing bending and shear strains.

SYMBOLS

a_n	normal acceleration, g units
b	airplane wing span, ft
E	modulus of elasticity, lb/sq in.
G	modulus of rigidity, lb/sq in.
g	acceleration due to gravity, 32.2 ft/sec^2
I	section moment of inertia, in.^{4}
J	polar moment of inertia, in.^{4}
q	dynamic pressure, $\frac{\rho V^2}{2}$, lb/sq ft
V	true airspeed, ft/sec
y	distance along span measured perpendicular to center line, ft
ρ	density of air, slugs/cu ft

σ root-mean-square deviation

σ_F root-mean-square deviation for flexible airplane

σ_R root-mean-square deviation for rigid airplane

AIRPLANE AND INSTRUMENTATION

A photograph of the test airplane is shown in figure 1. The only changes in the configuration of the standard airplane were the addition of a boom that was faired into the nose of the airplane for measuring flight speed and an external canopy mounted on top of the fuselage to house some of the instruments. (See figs. 1 and 2.) Some of the physical characteristics and dimensions of the airplane are listed in table I. The estimated wing and fuselage weight distributions for the tests are given in figures 3(a) and 3(b), respectively. All the fuel is carried in tanks located within the fuselage as shown in figure 3(b). Figure 3(c) shows the calculated wing bending stiffness distribution and the experimental wing torsional stiffness distribution as obtained from the manufacturer. It should be noted that the wing stations in figures 3(a) and 3(c) are measured along the elastic axis, whereas the stations in all subsequent figures are measured perpendicular to the airplane center line.

The basic instrumentation pertinent to the present paper consists of the following:

(1) An NACA air-damped recording accelerometer (response flat to about 10 cycles per second, accuracy ±0.0125g) was mounted close to the center of gravity of the airplane to measure normal acceleration.

(2) Twenty-two NACA oil-damped accelerometers (response flat to about 10 cycles per second, accuracy ±0.02g) were located at the points on the airplane wing and fuselage shown in figure 2.

(3) Electrical wire-resistance strain gages connected as four active gages in a bridge circuit were installed on the wing spars at the 10 locations shown in figure 2. The gages were not calibrated to measure actual load but served to give local strain indications only.

(4) An NACA airspeed-altitude recorder provided a record of airspeed and pressure altitude.

(5) NACA control position recorders recorded the aileron, rudder, and elevator displacements. These records were used as a check against the control movements being abrupt or large during the gust runs.

The film speed of the individual recorders was approximately 1/2 inch per second, and the film speed of the oscillographs that were used to record the outputs from the strain gages and oil-damped accelerometers was approximately 1 inch per second.

In addition to the recording instruments, cameras operating at a film speed of 1 frame every 2 seconds were focused on the fuel gages in order to determine the airplane weight at any point during the flight. All recordings were correlated by means of an NACA 1/10-second chronometric timer.

METHOD AND TESTS

Basic Approach

In the experimental determination of the effects of airplane flexibility on wing strains in rough air, it has been customary to compare the strains in rough air with the strains caused by the same loadings applied statically, such as those obtained in slow pull-up maneuvers. If the airplane flexibility does not seriously affect the airplane aerodynamic and stability characteristics, then this comparison provides a measure of the effects of flexibility. This condition seems to have been well approximated in earlier studies (refs. 1 to 4). If, on the other hand, the airplane flexibility involves appreciable wing twist, then this aeroelastic effect must also be considered. In the case of a swept-wing airplane, such aeroelastic effects due to the twist associated with the wing bending tend to be large and complicate the evaluation of the effects of flexibility.

The basic approach used in the present paper involves two types of comparisons. First, the actual measured strains in rough air are compared with the strains obtained for the test airplane by the static application of the same load. The strains for static application of loads are obtained from slow pull-up maneuvers at the same test condition. Since the effects of static aeroelasticity are reflected in both the rough-air and pull-up results, this comparison provides a measure of the purely dynamic or vibratory effects of airplane flexibility. Second, in order to obtain a measure of the effects of static aeroelasticity, the strains in rough air are also compared with the strains obtained by the static application of the same loads to a "rigid" airplane, that is, an airplane embodying no static aeroelastic effects. Inasmuch as static aeroelastic effects are a function of dynamic pressure, pull-up values at low or zero dynamic pressure are used to obtain the reference strains. The difference between the strains in rough air and strains obtained at the zero-dynamic-pressure reference condition provides a measure of the combined dynamic and static aeroelastic effects.

In both the gust and maneuver cases, the average airplane acceleration is used as a measure of the loading on the airplane. In the maneuver case, the loading is slow; therefore, the acceleration is approximately the same throughout the structure and, thus, any local acceleration may be used as a direct measure of the loading. In the gust case, however, vibratory modes are excited and the average airplane acceleration is different from the acceleration at local points on the airplane. As a consequence, the average airplane acceleration has to be approximated. The procedure used for this purpose is indicated subsequently.

Rough-Air Tests

Strain and acceleration data were obtained during a 4-minute test run at a Mach number of approximately 0.63 and an altitude of about 5,000 feet in clear-air turbulence. The average airplane weight was 113,000 pounds (which is a low weight condition for this airplane) and the airplane center of gravity was located at about 20 percent of the mean aerodynamic chord. The rough-air run was made with "hands off" control; that is, minor deviations of the airplane from the prescribed altitude and heading were not corrected by the pilot, and large deviations were corrected only by gradual control movements. This test procedure deviates from the conventional "stick free" case because the power-boost control system used on this airplane causes the control surfaces to be essentially "fixed" except for a pilot-controlled input.

Smooth-Air Tests

In order to determine the strain indications per g for the various gages under a quasi-steady loading condition, slow pull-up maneuvers were made in smooth air before and after the rough-air runs. Generally, these pull-ups were made at a higher altitude than the gust runs in order to obtain smooth air. Since the dynamic pressure differed for these pull-ups at the higher altitudes, runs were made at two Mach numbers, 0.65 and 0.35, and at two altitudes roughly 10,000 feet apart. The fairly wide range of dynamic pressure which was covered permitted the establishment of the variation in the strain indication per g with dynamic pressure and also permitted the determination of the strain indication per g at zero dynamic pressure. This value serves as a useful rigid reference value.

EVALUATION OF DATA AND RESULTS

As an indication of the general characteristics of the airplane strain and acceleration responses in rough air, sections of the measured

quantities for the rough-air run are shown in figure 4. The records indicate the vibratory character of the airplane response. In addition, a number of predominant frequencies are discernible in the various strain and acceleration histories. Samples of the records obtained in a typical pull-up are shown in figure 5. In contrast to the rough-air records, the response in a pull-up is smooth and regular and shows no evidence of the excitement of the airplane structural modes; the quasi-steady character of the load application for the pull-up maneuvers is thereby indicated.

The data-reduction procedure involved the following steps:

(1) An evaluation of the strains experienced in rough air

(2) An evaluation of the associated average airplane acceleration in rough air

(3) An evaluation of the steady strains per unit acceleration in the pull-up maneuvers

The results obtained in the data-reduction steps (1) to (3) are then used to obtain overall measures of the aeroelastic effects in the form of amplification factors. The procedures used for each of these steps and the results obtained are described in order in the following sections. The recorded quantities were evaluated at 0.05-second intervals along the time histories. All records were read and processed with automatic digital computing equipment.

Rough-Air Strains

In previous investigations, a "selected peak" type of evaluation was used to present the data. (See, for example, ref. 4.) In an evaluation of this type, judgment was frequently necessary to match the peak nodal acceleration and the associated peak strains. This difficulty may be avoided by eliminating the timewise association and comparing directly the overall strain time histories in terms of the number of peaks of a given magnitude. Figure 6 shows the procedure used to obtain this count of the number of peaks. As shown in figure 6, only one peak is counted between consecutive intersections of the trace with the trace position for steady level flight. A threshold depending on gage sensitivity must also be exceeded and, for the sketch of the record portion shown in figure 6, four readings at points a, b, c, and d were made. These peak readings were then used to determine the cumulative frequency distributions. In addition to the determination of the cumulative peak distributions, the time histories were used to obtain the root-mean-square strains.

Inasmuch as the strain per g under steady loads varied widely among gages, a normalizing procedure was used in order to simplify comparisons of the strain counts for different stations. The normalizing procedure consisted of dividing all strain indications (record deflection minus mean deflection) by the pull-up slope (Deflection/g) in steady pull-ups for the individual gages. The resulting strain values are accordingly converted to units of equivalent acceleration as was done in reference 4. The cumulative distributions of strain peaks in acceleration units for the various strain-gage stations are given in figures 7 and 8 for both the front-spar and rear-spar stations. Figure 7 presents the bending-strain results and figure 8 gives the shear-strain results.

Average Airplane Acceleration in Rough Air

The determination of the average airplane acceleration for the gust condition for the present airplane posed a number of problems. In previous flight-test studies on unswept-wing airplanes (refs. 1 to 4), the procedure was based on the use of the measured accelerations at the nodal points of the fundamental wing bending mode for the gust-loading condition. The location of the nodal point of the fundamental wing bending mode in these cases was not difficult since the bending mode was usually at a much higher frequency than the airplane short-period mode. The effects of the airplane higher vibrational frequencies at the nodal points of the fundamental wing bending mode were usually evident and it was necessary to eliminate them by fairing. For the present airplane, this procedure did not seem feasible. Two difficulties arose: First, the location of the nodes from the flight recordings of acceleration at various locations along the wing did not appear to be practical since the fundamental wing bending frequency could not be clearly distinguished from the airplane short-period pitching frequency. Second, a correction to the wing accelerations for the airplane pitching motions would most likely be required because of the longitudinal distance between the nodal points of the swept wing and the airplane center of gravity.

An inspection of the records indicated that the acceleration at the center of gravity would approximate the average airplane acceleration. Also, from a consideration of the mass distribution of the airplane and the shape of the first mode in bending, the nodal points of the fundamental wing bending mode were expected to be fairly close inboard. A short section of record was used as a check on the reliability of using the acceleration at the center of gravity as a measure of the rough-air loading. The procedure used was the averaging of the acceleration over the entire airplane mass and was accomplished by summing the products of the local accelerations and associated masses and dividing by the total mass of the airplane. Twenty-two local acceleration measuring stations were used (six stations along the fuselage and 16 locations along the front and rear spars of the wing as shown in fig. 2). The airplane

mass distribution, as given in figures 3(a) and 3(b), was subdivided in such a way as to associate portions of the mass of both the wing and fuselage with the nearest accelerometer station. A time history of this averaged airplane acceleration for approximately 10 seconds of rough-air flight is shown in figure 9(a).

The center-of-gravity acceleration exhibited considerable high-frequency "hash" of frequencies above 5 cycles per second associated with the higher structural modes and not reflected in the airplane acceleration. Consequently, these higher frequencies were faired as illustrated by the sample record sections in figure 9(b). The faired center-of-gravity acceleration is also shown in figure 9(a) for comparison with the airplane acceleration. In general, good agreement is noted in figure 9(a) between the time histories of the faired center-of-gravity acceleration and the airplane acceleration based on the 22 accelerometers, although some discrepancy may be noted for individual peaks. Comparison of the overall counts of the peak accelerations made for the same samples showed good agreement, however. The power spectrum of the faired normal acceleration at the center of gravity was also determined and indicated some effects of the first bending mode. However, these effects were small and were estimated to yield a 5-percent increase in the acceleration, which is considered negligible for present purposes. Accordingly, the faired center-of-gravity acceleration was used as a direct measure of the airplane loads. Peak counts of the faired center-of-gravity accelerations were then made for the 4-minute gust run in a manner similar to the counts of rough-air strain, as illustrated in figure 6. The resulting cumulative distributions of faired center-of-gravity-acceleration peaks are then given in figures 7 and 8 for comparison with the peak counts of rough-air strain.

Pull-Up Maneuver Strains

As indicated in a previous section of this paper, the quasi-static strain indications per g for slow pull-up maneuvers obtained at the several stations along the wing varied considerably with dynamic pressure. This variation was attributed to an inboard shift in center of pressure of the additional load resulting from increasing load alleviation outboard due to wing twist as dynamic pressure increased.

The variation of strain indication with g was linear for the various gages and accordingly the slope was used as a measure of strain indication per g for the individual pull-up maneuvers. A typical plot of the strain indication per g against dynamic pressure is presented in figure 10 for wing station 414. Each datum point on the plot represents the slope of the strain variation with acceleration for a single pull-up maneuver. Other strain-gage locations along the wing give similar results; some locations yielded somewhat more rapid variations of

strain per g with dynamic pressure than others. The values have all been adjusted for slope change due to change in airplane weight and are shown plotted in figure 10 for the average airplane weight during the gust run.

If the data for the two gages of figure 10 are extrapolated to a dynamic pressure of zero, as shown by the solid lines, a value of strain per g is obtained and is assumed to correspond to that which would be obtained if no load alleviation due to wing twist had occurred. (In most cases, the variation of strain indication per g with dynamic pressure appeared to be linear; therefore, a linear extrapolation was made.) Thus, two pertinent values of strain per g are obtained for each gage, one for a condition where quasi-static twist effects are eliminated (zero dynamic pressure) and the other at the dynamic pressure of the gust run (484 pounds per square foot). These two sets of reference strains are given in table II and are used subsequently to obtain amplification factors.

Amplification Factors

For the swept-wing airplane of the present investigation, amplification factors are determined in two different ways. These two amplification factors are based on the two sets of reference strains given in table II.

Amplification factors (with the strain per g at the test dynamic pressure of the gust run as the reference condition) may be obtained from figures 7 and 8 at any strain level within the reliable range of the curves by taking the ratio of the value of strain in g units from the curve for the flexible airplane (see point A of fig. 7, for example) to the value in g units from the curve of the reference airplane acceleration (for example, point B of fig. 7). It can be seen that the amplification factor varies with the cumulative frequency chosen.

The ratio of values from the curve for the flexible airplane to those from the curve for the reference airplane is high at high values of cumulative frequency (low strain levels) and decreases with decreasing cumulative frequency (high strain levels). It can be shown that this ratio approaches the ratio of root-mean-square values at high levels of strain. The actual strain level that is important would appear to depend upon the nature of the application.

For present purposes, two values of amplification factors have been obtained for each of the two reference conditions; one is at a level of strain of 2σ for the flexible airplane. For example, this condition leads to point A in figure 7(c) and to the amplification factor given by A/B. The other value of amplification factor is one determined from the ratio

of the root-mean-square values (strain to airplane acceleration). Amplification factors for both the bending and shear strains were determined for each of the eight strain-gage locations and are given in table II.

As indicated in the section entitled "Rough-Air Strains," the cumulative distributions of strain peaks presented in figures 7 and 8 were "normalized," or converted to acceleration units, by use of the reference strain per g obtained at the dynamic pressure of the gust run (484 pounds per square foot). The amplification factors obtained from these figures are, of course, for this reference condition. Similar figures were obtained for the zero-dynamic-pressure reference condition by the conversion of the cumulative distributions of strain peaks to acceleration units with the use of the appropriate reference strain indication per g. Such figures are not presented, but the amplification factors determined for this reference condition are given in table II. The amplification factors obtained for both reference conditions are shown in figures 11 and 12 as functions of wing station for the bending and shear strains, respectively. It is to be noted in figure 12 that for the front-spar gage at station 252 for both reference conditions and for the front-spar gage at station 54 at the zero-dynamic-pressure reference condition, reliable values of strain per g in pull-ups could not be obtained and, therefore, the amplification factors for shear strain at these stations are not shown.

DISCUSSION

Inasmuch as the method used herein for obtaining amplification factors is based on a comparison of frequency distributions and differs from that used in references 2 and 4, a comparison has been made of the magnitude of the amplification factors obtained by the two methods. For this comparison, amplification factors based on the selected-peak method used in previous studies were determined for several of the strain channels of the present data. In general, the amplification factors obtained on this basis were in good agreement with those obtained at the level of $2\sigma_F$ (fig. 7). Figure 13 shows an example of the results obtained by the selected-peak method. The least-squares line through the data is also shown and yields an amplification factor of 2.68 for this case. The value obtained in this case from the frequency distributions was 2.72 as indicated in table II for wing station 414, front spar. Thus, the ratio of "flexible" to "reference" at $2\sigma_F$ yields amplification factors which are in good agreement with those obtained from the selected-peak method. Amplification factors based on the ratio of root-mean-square values, however, are somewhat lower than those given by either the selected-peak or $2\sigma_F$ method.

Bending Strains

A summary of the amplification factors obtained for the bending strains is given in figure 11 and table II. The results for the front spar (fig. 11(a)) show that amplification factors based on the root-mean-square values for the test value of dynamic pressure (the broken line with the circled points) increase from a value of 1.07 at the root to a value of 2.00 at station 414 and then decrease somewhat at the most outboard station. The amplification factors based on the strain values at $2\sigma_F$ show a similar trend but have consistently higher values than those previously mentioned; the value at the root is 1.16 and increases to 2.72 at station 414. The same general situation, except for differences in the actual values, is seen to exist for the rear spar (fig. 11(b)). Thus, in general, the amplification factors of the strains appear to be small at the root but increase to very large values at the outboard stations.

The results shown in figure 11 for the zero-dynamic-pressure reference condition provide a measure of the total amplification of the strains relative to a hypothetical rigid airplane, that is, an airplane embodying no static aeroelastic or twist effects. The amplification factors obtained on this basis are a measure of the combined effects of dynamic amplification and static alleviation due to wing twist. For this reason, a significant reduction exists in the magnitude of the amplification factors obtained. For example, at the root station of the front spar, the amplification factor based on the ratio of the root-mean-square values is reduced from 1.07 for the gust-dynamic-pressure reference to a value of 0.86 for the zero-dynamic-pressure reference. Since the latter amplification factor is less than 1, a net reduction of the strain per g in gusts as compared with the strain per g expected in a pull-up maneuver of the hypothetical rigid airplane is implied. At station 414, the reduction is from 2.00 to 1.26. Thus, the overall effects of flexibility as represented by amplification factors that include both dynamic and static aeroelasticity are considerably less than the amplification factors which include only the dynamic effects.

Shear Strains

The results for the rear-spar shear strains are similar to those for the bending strains and show relatively small amplifications at the root and large amplifications at the outboard stations. The results for the front spar show some variations from this general pattern with larger shear-strain amplifications at the root than those for the bending strains. The reason for the deviation of the results at the front-spar shear gages from the general pattern is not clear, but the discrepancy may be associated with the fact that the wing twist arising from the inertia loads of the inboard nacelle has greater effects on the front-spar root station.

The amplification factors for the shear strains shown in figure 12 are, in general, considered less representative of a given region than those for the bending strains because of the greater local variations normally encountered for shear strains in an airplane structure.

CONCLUDING REMARKS

A flight investigation in rough air was undertaken on a flexible swept-wing airplane to determine the effects of flexibility on the wing bending and shear strains. For the airplane tested, both dynamic and static aeroelastic effects have a large influence on the bending and shear strains across the span. The bending-strain amplification factors reflecting the dynamic effects alone are smallest at the root, where the values are 1.20 to 1.30, and increase rapidly along the span to a value as high as 2.72. The shear-strain amplifications show the same general pattern but are less consistent between front and rear spars than those for the bending gages because of larger localized strain effects on the web-mounted shear gages. Amplification factors based on the strain per unit acceleration in pull-ups extrapolated to zero dynamic pressure provide a measure of the combined static and dynamic aeroelastic effects and are substantially lower than those determined for dynamic aeroelastic effects alone. For the bending strains, these strain amplification factors were negligible at the root and increased to a value of about 1.50 at the outboard stations. The shear-strain results show similar trends.

The relatively large amplification factors noted in the present study and their wide variation with spanwise location, particularly at the outboard stations, indicate that a detailed analysis of the aeroelastic effects are required for the successful prediction of gust strains. With regard to the prediction of bending strains, it should be noted that at the root stations the strain records are of an essentially low-frequency nature and thereby reflect largely rigid airplane motions and bending in the first mode, which is at approximately 1.5 cycles per second. At the outboard stations, the strain records indicate considerably more evidence of the higher frequencies, suggesting that the higher vibrational modes become more important in regard to strains at these locations in the present case as was the case in NACA Technical Note 4071. A reliable dynamic analysis for bending-strain calculations, at these outboard stations particularly, would thus apparently require the considerations of these higher vibrational modes.

The successful analysis of the shear strains at all stations, which have frequency characteristics similar to the bending strains at the outboard stations, would also appear to require the consideration of higher vibrational modes in the analysis.

Langley Aeronautical Laboratory,
National Advisory Committee for Aeronautics,
Langley Field, Va., June 26, 1957.

REFERENCES

1. Shufflebarger, C. C., and Mickleboro, Harry C.: Flight Investigation of the Effect of Transient Wing Response on Measured Accelerations of a Modern Transport Airplane in Rough Air. NACA TN 2150, 1950.

2. Mickleboro, Harry C., and Shufflebarger, C. C.: Flight Investigation of the Effect of Transient Wing Response on Wing Strains of a Twin-Engine Transport Airplane in Rough Air. NACA TN 2424, 1951.

3. Mickleboro, Harry C., Fahrer, Richard B., and Shufflebarger, C. C.: Flight Investigation of Transient Wing Response on a Four-Engine Bomber Airplane in Rough Air With Respect to Center-of-Gravity Accelerations. NACA TN 2780, 1952.

4. Murrow, Harold N., and Payne, Chester B.: Flight Investigation of the Effect of Transient Wing Response on Wing Strains of a Four-Engine Bomber Airplane in Rough Air. NACA TN 2951, 1953.

5. Houbolt, John C., and Kordes, Eldon E.: Structural Response to Discrete and Continuous Gusts of an Airplane Having Wing-Bending Flexibility and a Correlation of Calculated and Flight Results. NACA Rep. 1181, 1954. (Supersedes NACA TN 3006; also contains essential material from TN 2763 and TN 2897.)

6. Press, Harry, and Houbolt, John C.: Some Applications of Generalized Harmonic Analysis to Gust Loads on Airplanes. Jour. Aero. Sci., vol. 22, no. 1, Jan. 1955, pp. 17-26, 60.

7. Shufflebarger, C. C., Payne, Chester B., and Cahen, George L.: A Correlation of Results of a Flight Investigation With Results of an Analytical Study of Effects of Wing Flexibility on Wing Strains Due to Gusts. NACA TN 4071, 1957.

TABLE I.- PERTINENT PHYSICAL CHARACTERISTICS AND DIMENSIONS OF TEST AIRPLANE

Total wing area, sq ft	1,428
Wing span, ft	116
Wing aspect ratio	9.43
Wing thickness ratio, percent	12
Wing taper ratio	0.42
Wing mean aerodynamic chord, in.	155.9
Wing sweepback (25-percent-chord line), deg	35
Total horizontal-tail area, sq ft	268
Horizontal-tail span, ft	33
Horizontal-tail mean aerodynamic chord, in.	102.9
Horizontal-tail sweepback (25-percent-chord line), deg	35
Airplane weight, lb	100,000 to 120,000

TABLE II.- AMPLIFICATION FACTORS OF STRAIN

Wing station	Spar	Bending-strain indication				Shear-strain indication			
		Pull-up factor (a)	$2\sigma_F$ level (b)	Amplification factor		Pull-up factor (a)	$2\sigma_F$ level (b)	Amplification factor	
				Values at $2\sigma_F$ level	$\frac{\sigma_F}{\sigma_R}$			Values at $2\sigma_F$ level	$\frac{\sigma_F}{\sigma_R}$
Reference q = 484 lb/sq ft									
54	Front	0.469	0.220	1.16	1.07	0.150	0.362	2.15	1.77
54	Rear	.809	.225	1.32	1.10	.496	.202	1.12	.99
252	Front	.448	.253	1.45	1.23	-----	-----	----	----
252	Rear	.434	.262	1.53	1.28	.186	.302	1.89	1.47
414	Front	.416	.410	2.72	2.00	.320	.277	1.62	1.35
414	Rear	.511	.352	2.26	1.72	.160	.392	2.42	1.91
572	Front	.183	.324	2.31	1.58	.427	.194	1.21	.95
572	Rear	.251	.297	1.97	1.45	.163	.385	2.00	1.88
Reference q = 0 lb/sq ft									
54	Front	0.582	0.178	0.93	0.86	-----	-----	----	----
54	Rear	1.052	.173	1.01	.84	0.550	0.183	1.01	0.89
252	Front	.671	.169	.97	.82	-----	-----	----	----
252	Rear	.608	.187	1.09	.92	.339	.165	1.04	.81
414	Front	.660	.258	1.71	1.26	.478	.185	1.08	.91
414	Rear	.653	.276	1.77	1.35	.217	.288	1.78	1.41
572	Front	.291	.203	1.45	.99	.579	.143	.89	.70
572	Rear	.411	.182	1.20	.89	.232	.271	1.40	1.32

[a]Record deflection, inches per g (adjusted for changes in system voltage).

[b]Converted to equivalent g units by use of pull-up factor.

Figure 1.- Photograph of test airplane. L-86692

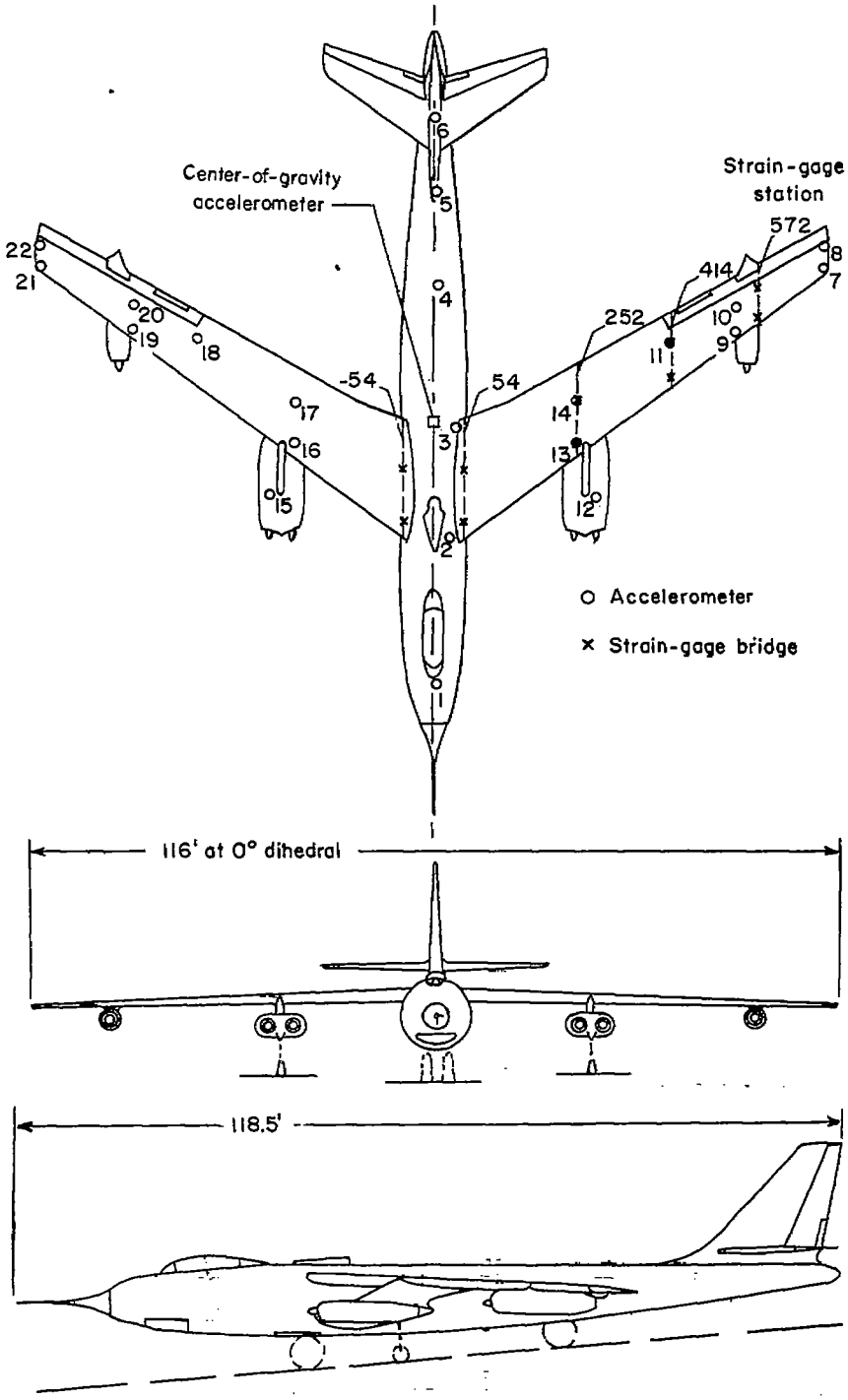

Figure 2.- Three-view drawing of test airplane.

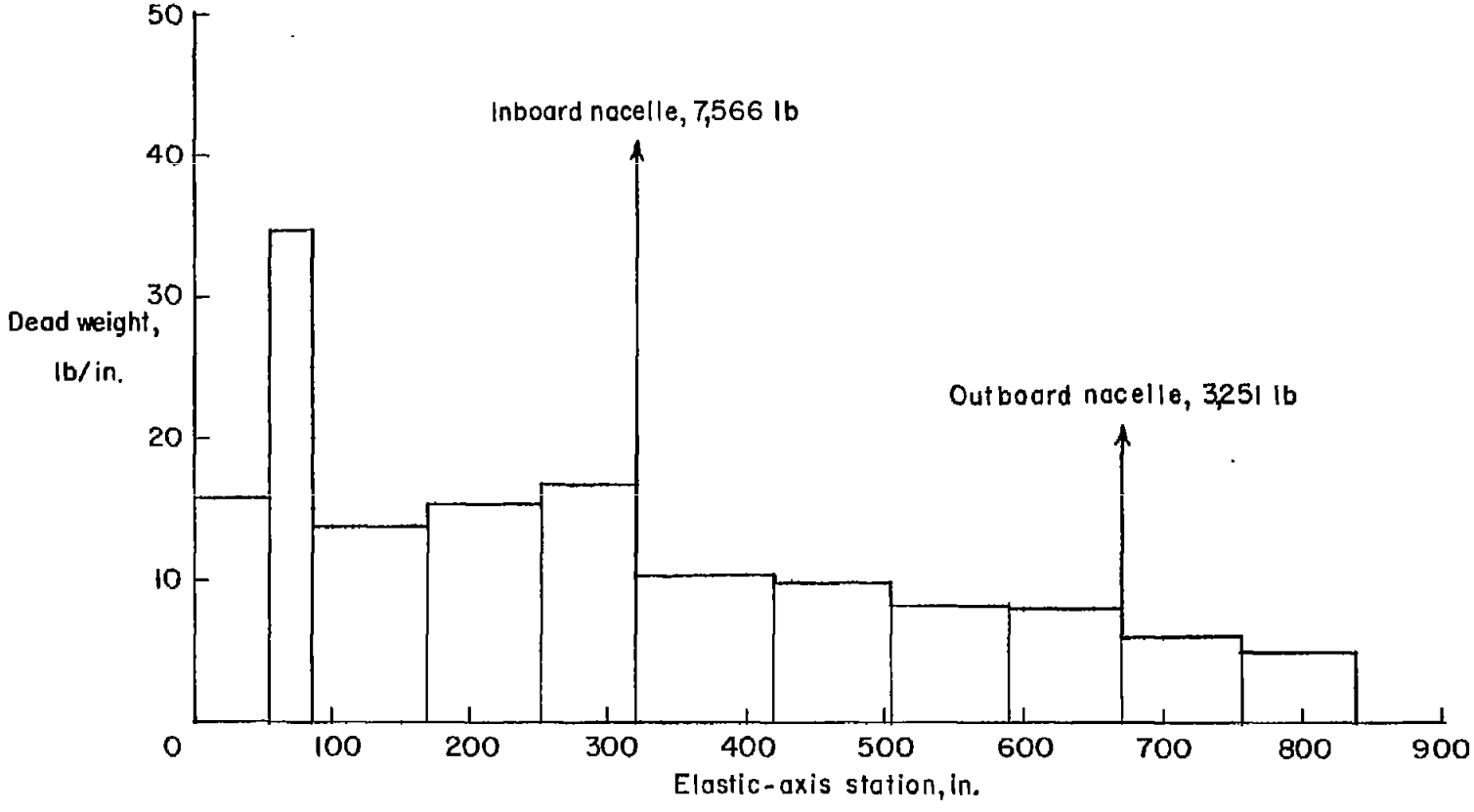

(a) Wing dead-weight distribution.

Figure 3.- Airplane weight and stiffness distributions.

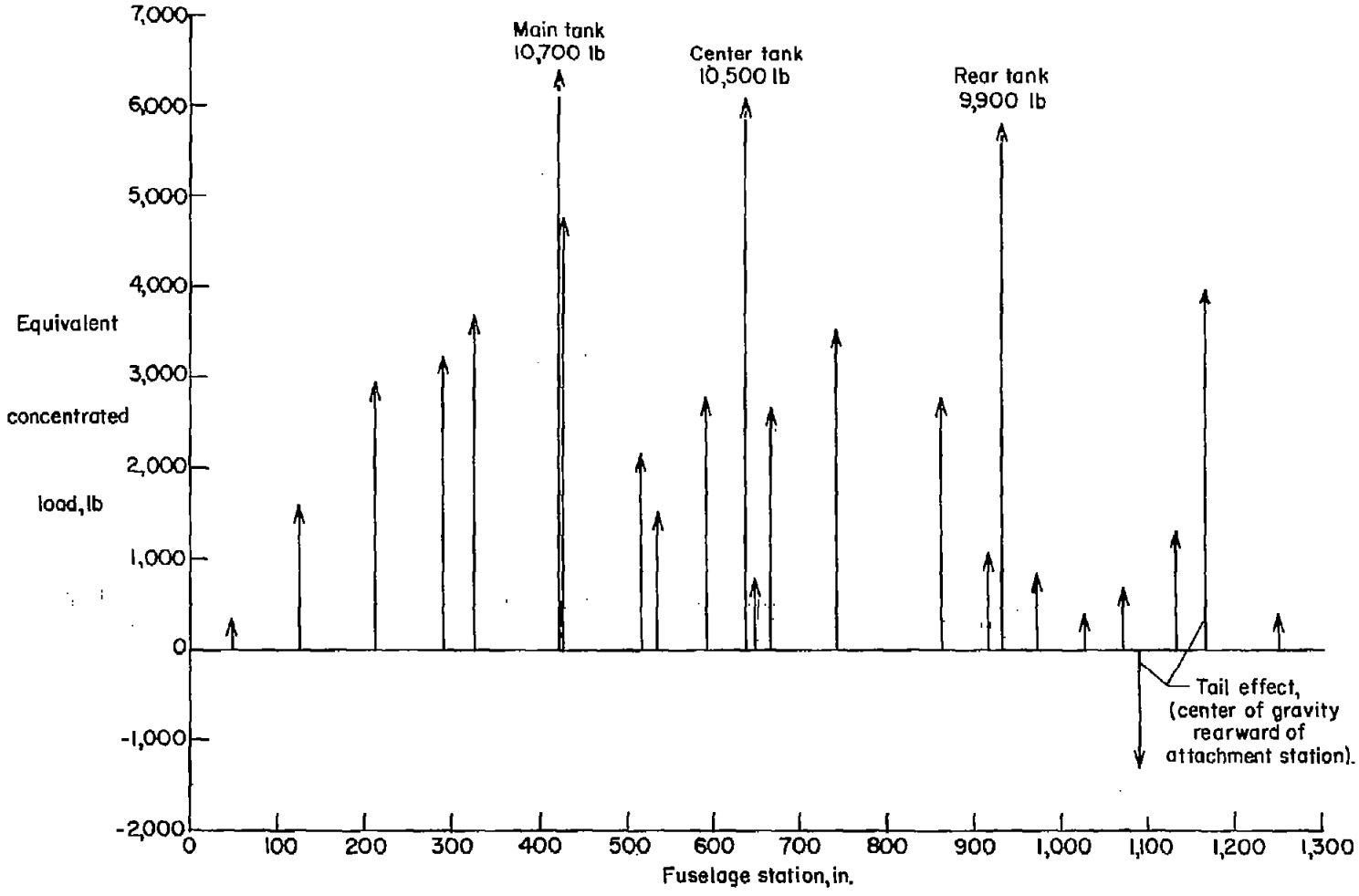

(b) Approximate weight distribution of the fuselage including weight of the pilots, instruments, and average fuel for the gust run.

Figure 3.- Continued.

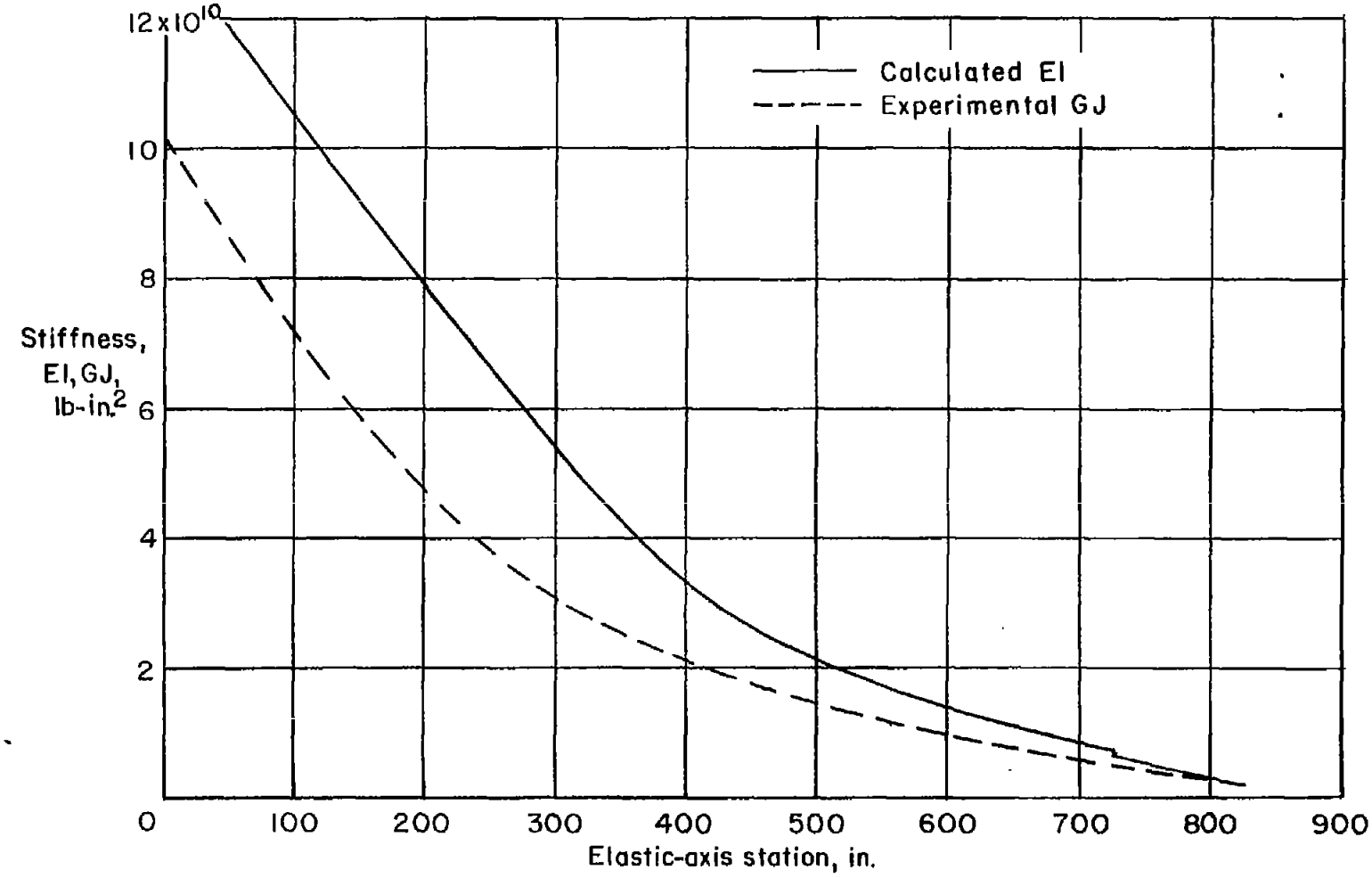

(c) Bending and torsional stiffness distributions of wing.

Figure 3.- Concluded.

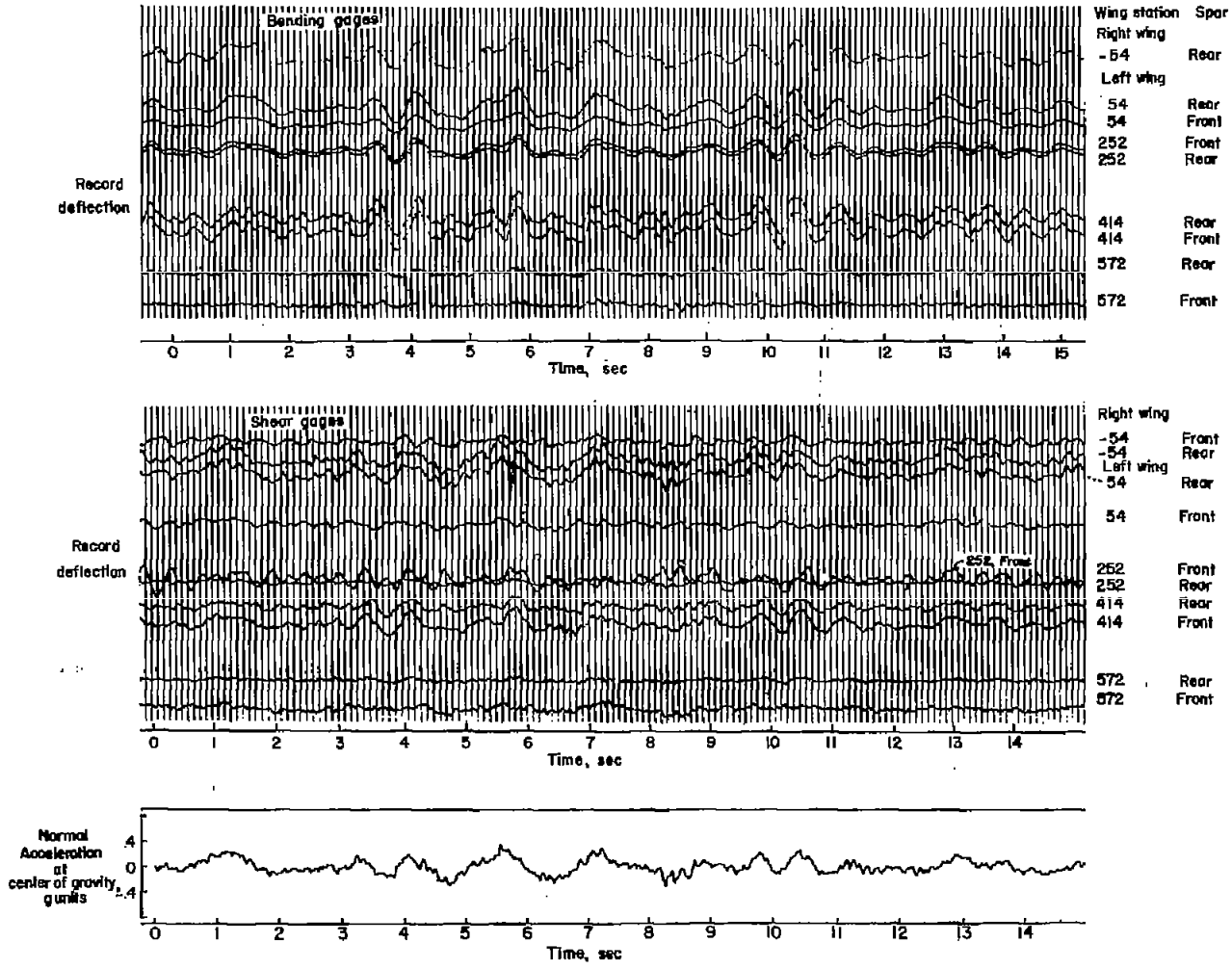

(a) Wing strains and acceleration at center of gravity.

Figure 4.- Sample time histories in rough air.

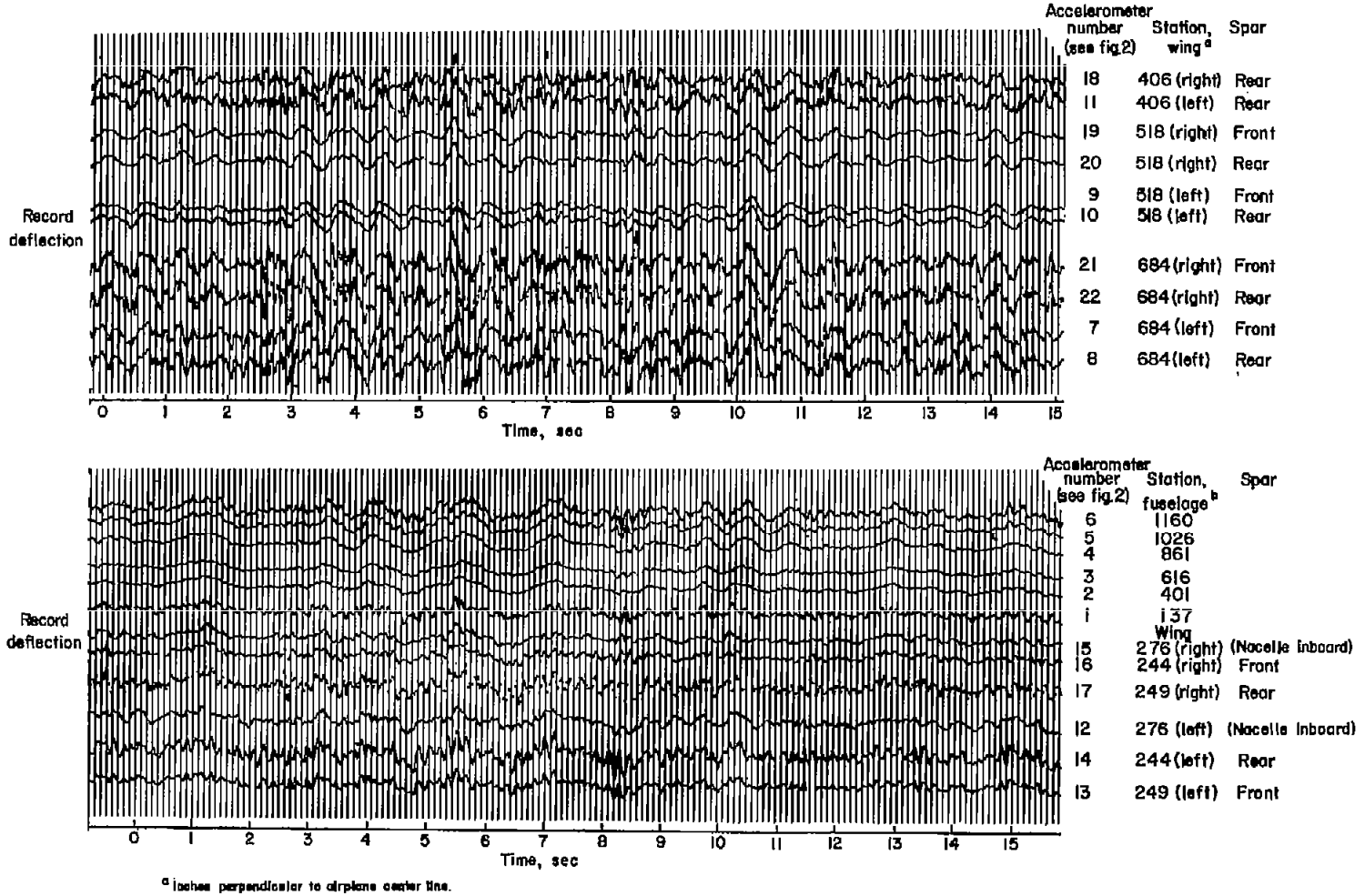

[a] Inches perpendicular to airplane center line.

[b] Inches from manufacturer's reference datum in nose.

(b) Local wing and fuselage accelerations.

Figure 4.- Concluded.

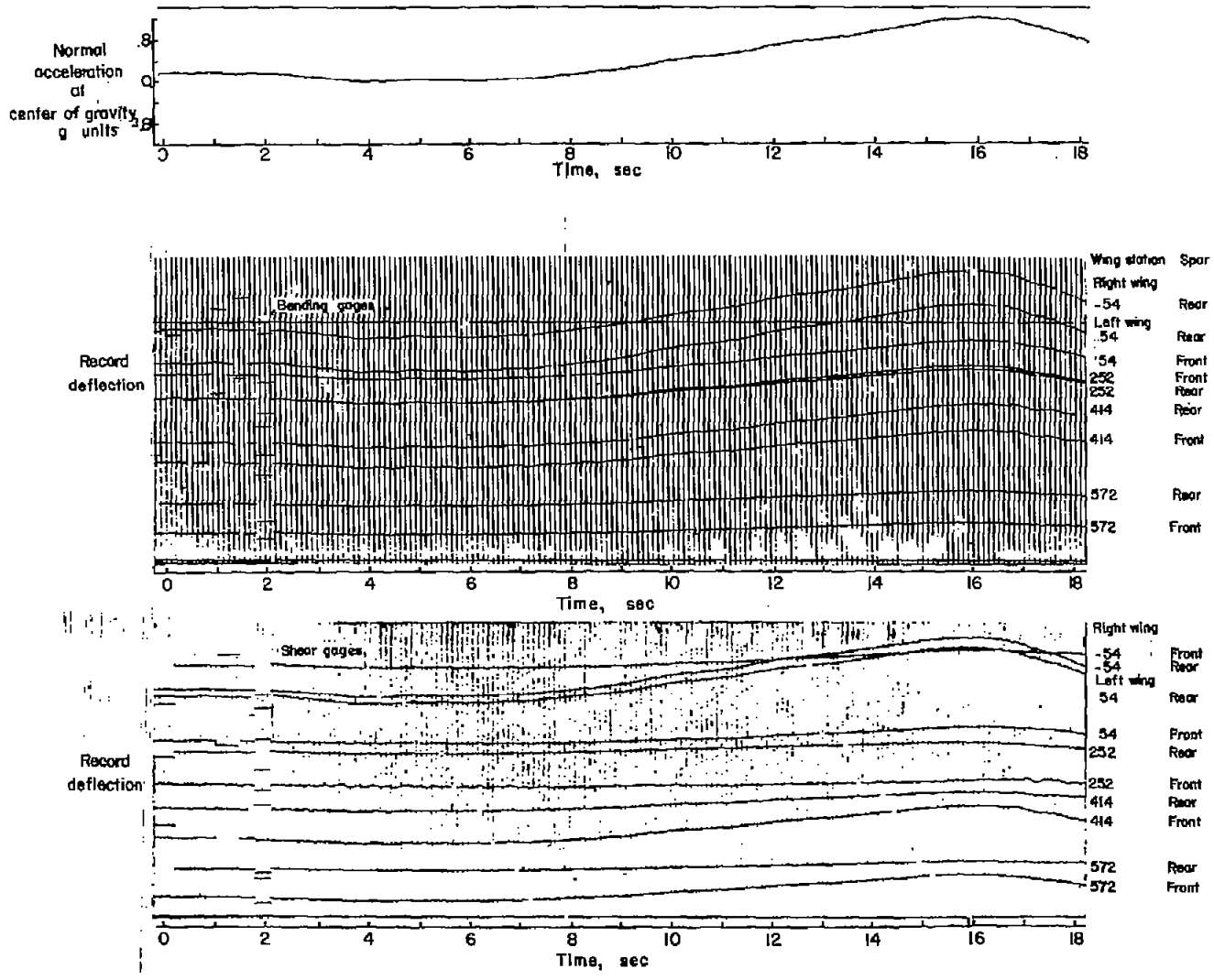

Figure 5.- Time histories of wing strains and acceleration at center of gravity in typical pull-up.

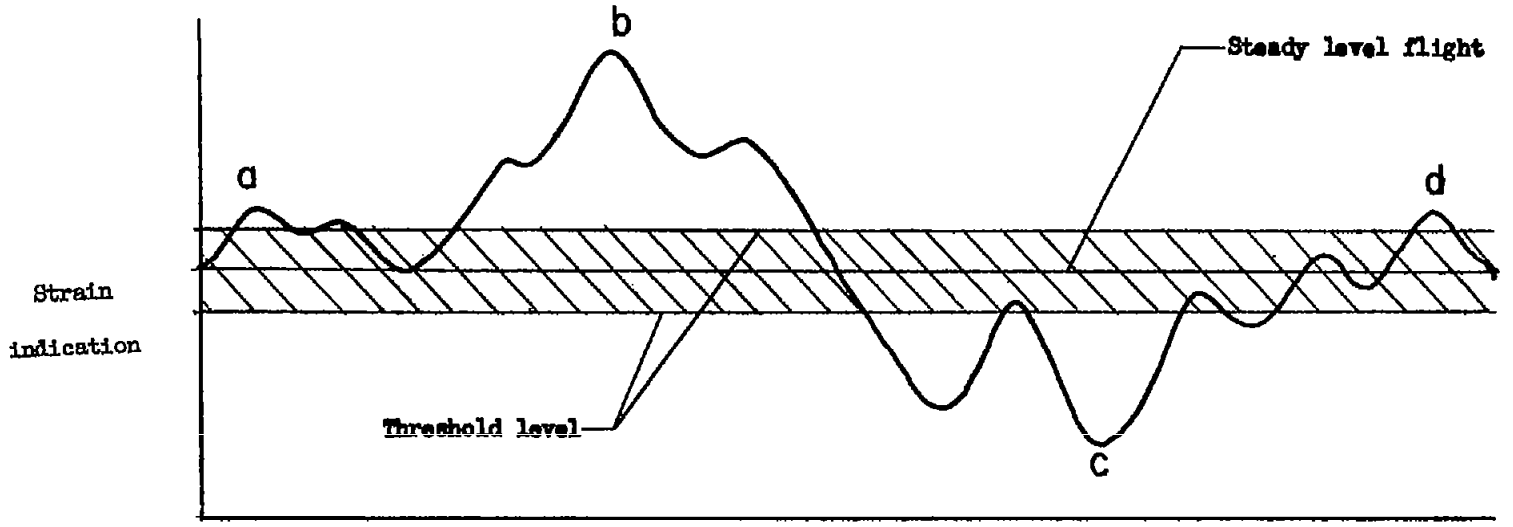

Figure 6.- Illustrative strain time history showing method of count.

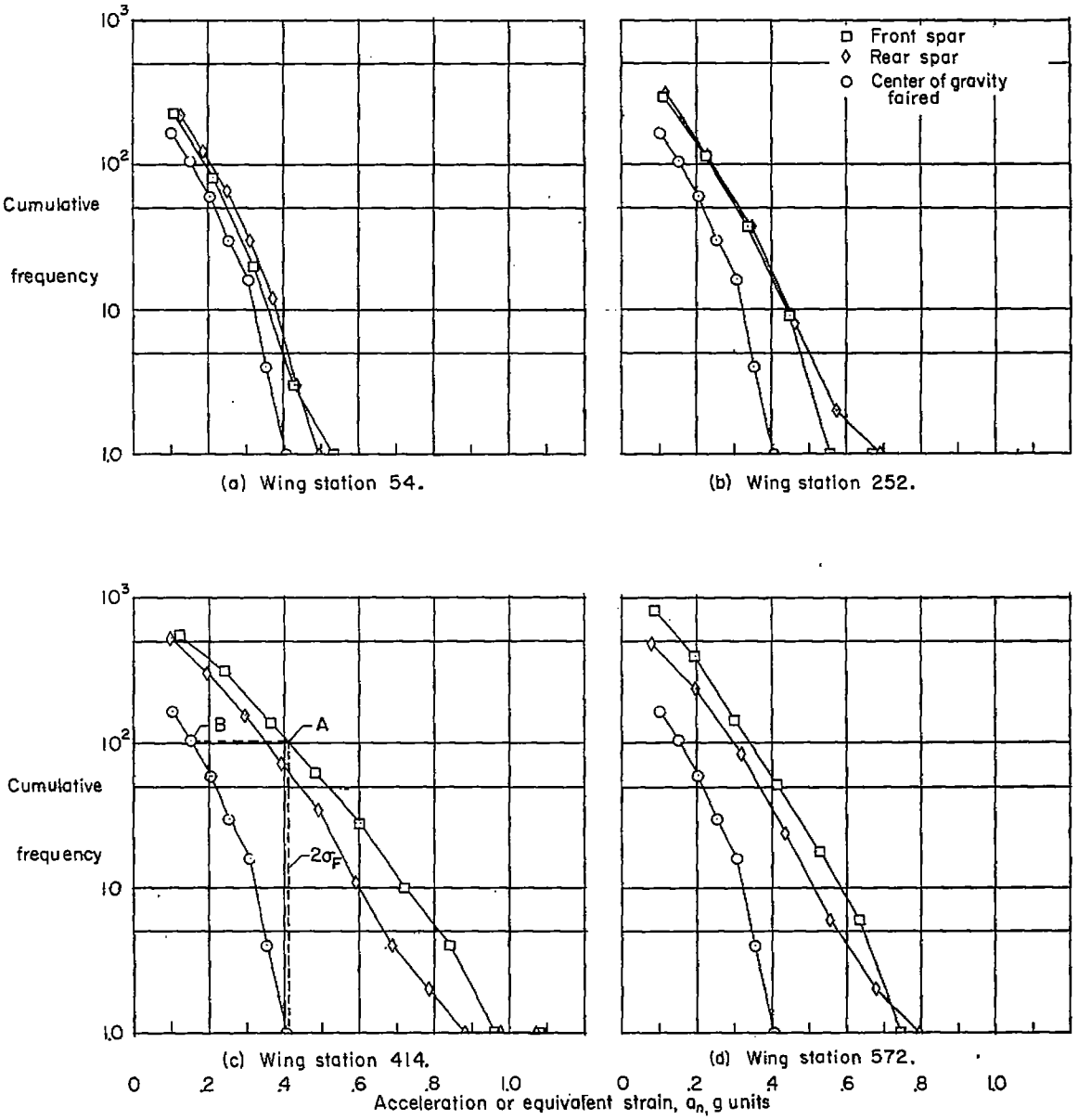

Figure 7.- Cumulative frequency distributions of faired center-of-gravity acceleration and bending strains in g units.

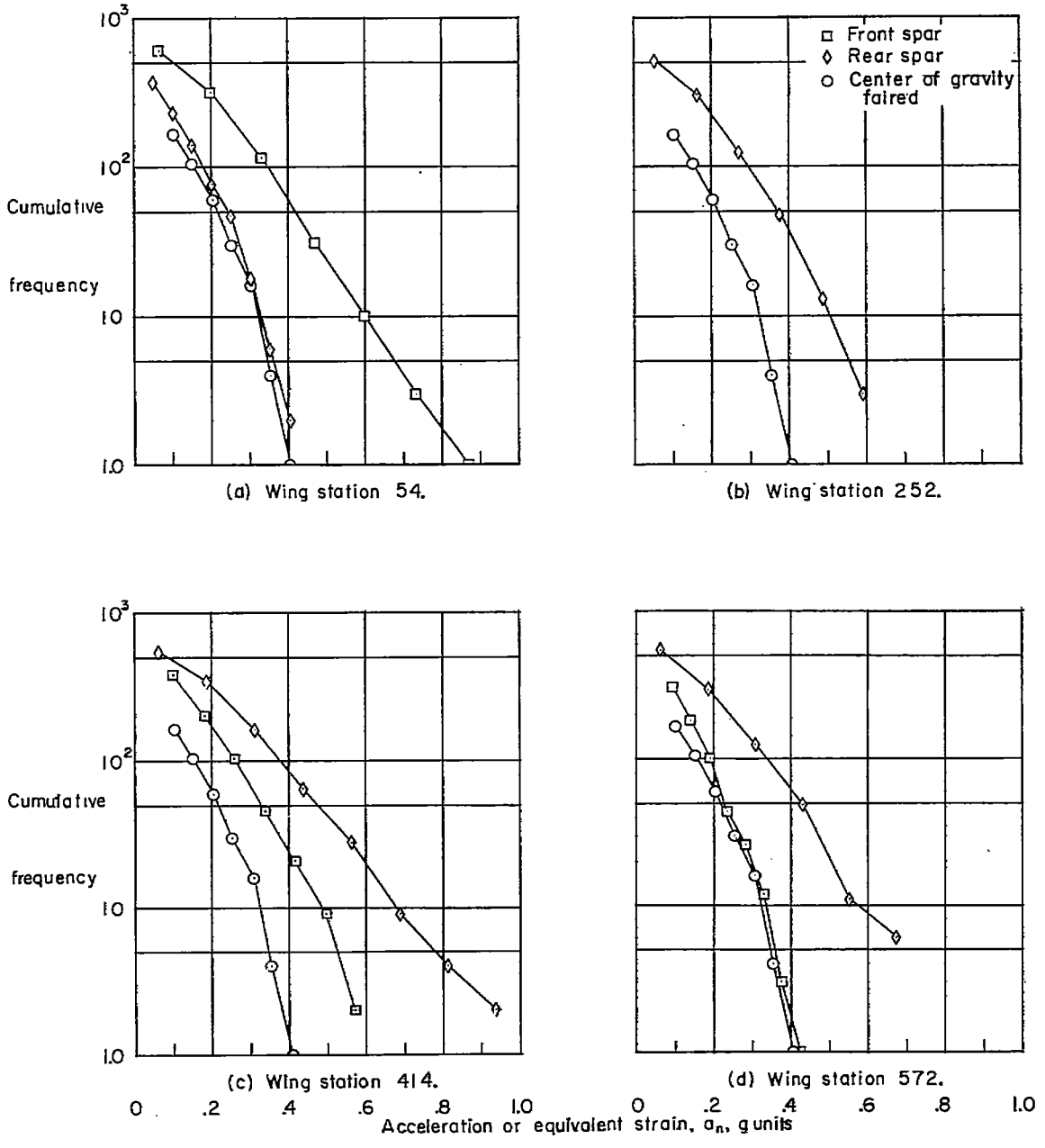

Figure 8.- Cumulative frequency distributions of faired center-of-gravity acceleration and shear strains in g units.

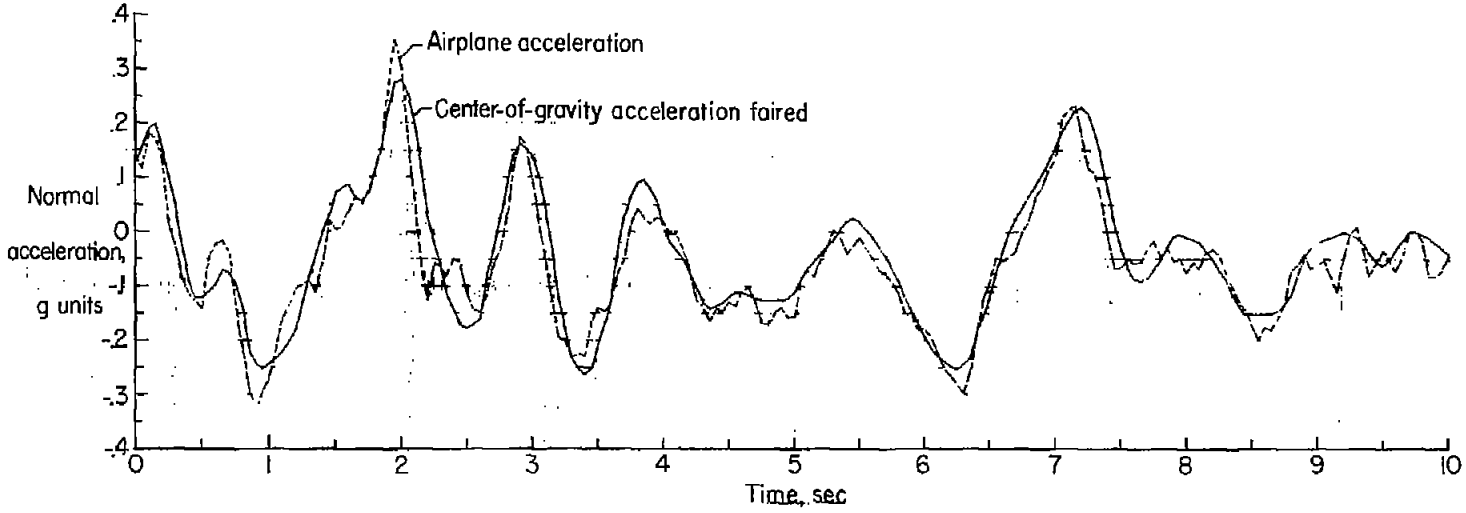

(a) Airplane acceleration.

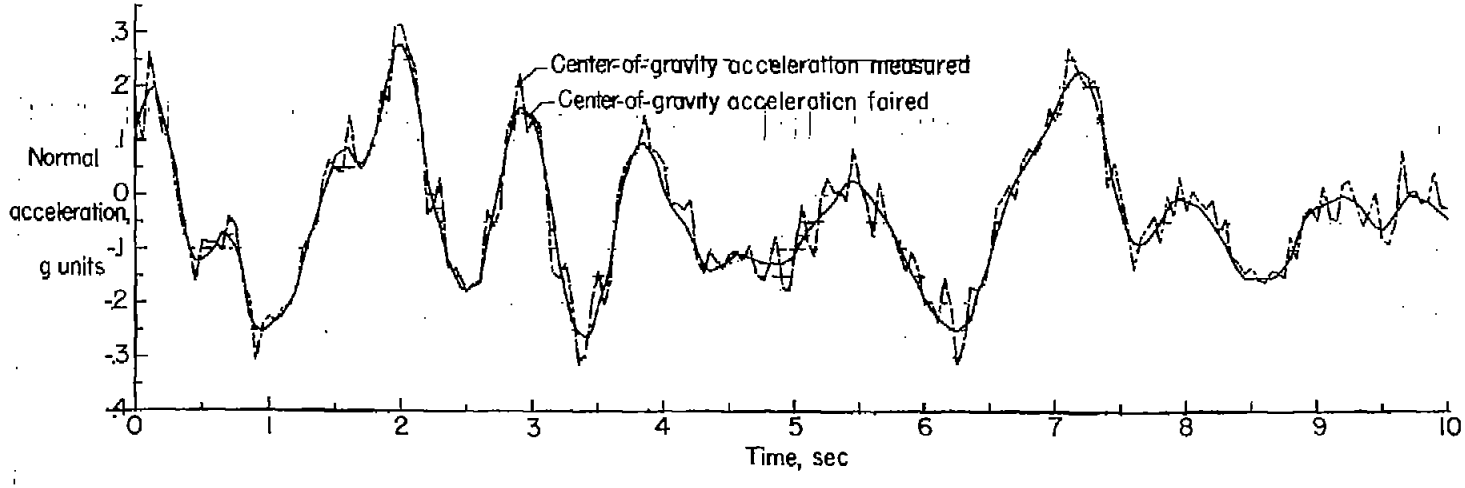

(b) Center-of-gravity acceleration.

Figure 9.- Comparison of airplane acceleration computed from 22 acceleration time histories, and faired measurement of acceleration at airplane center of gravity.

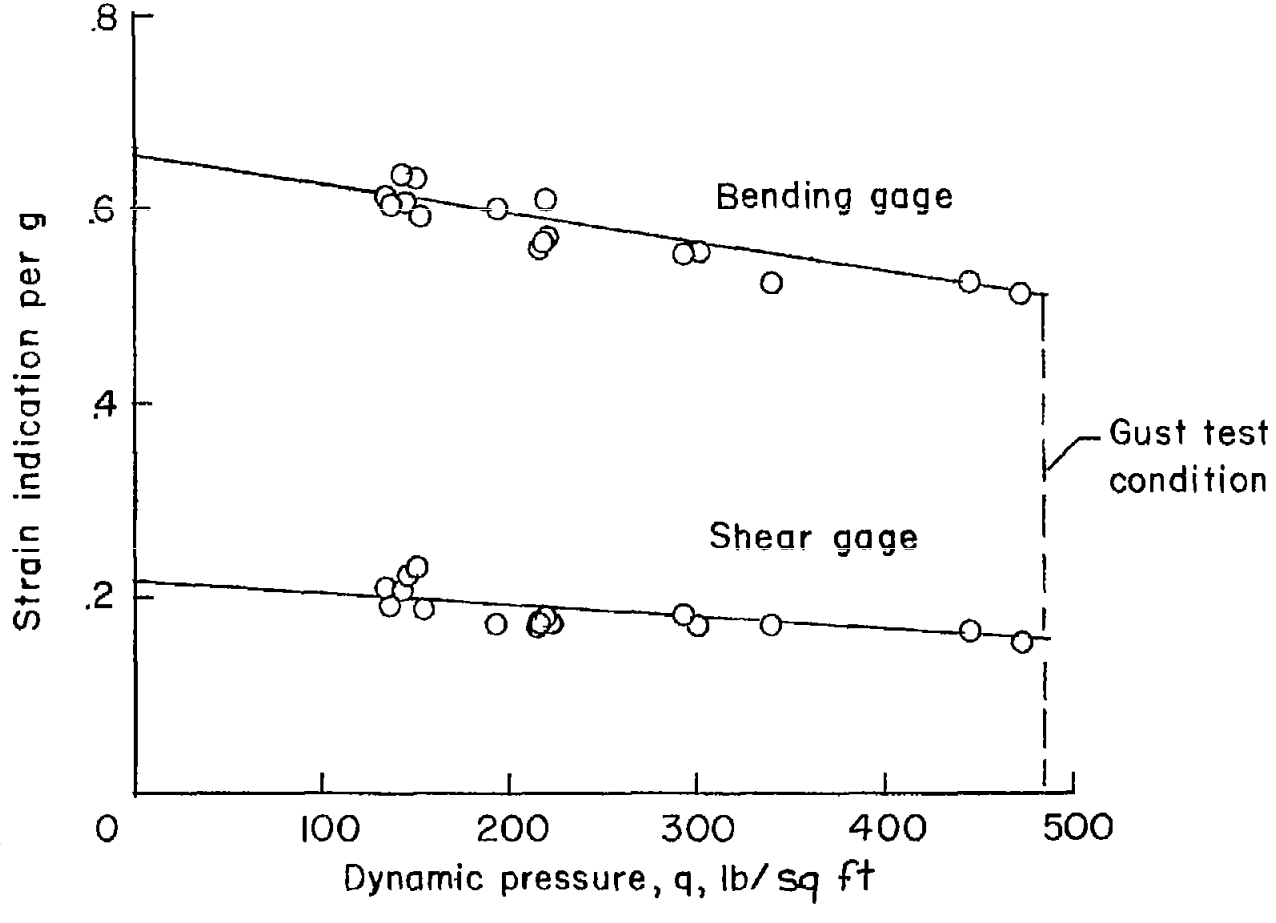

Figure 10.- Typical values of strain indication per g in a pull-up maneuver plotted against dynamic pressure. Wing station 414; rear spar.

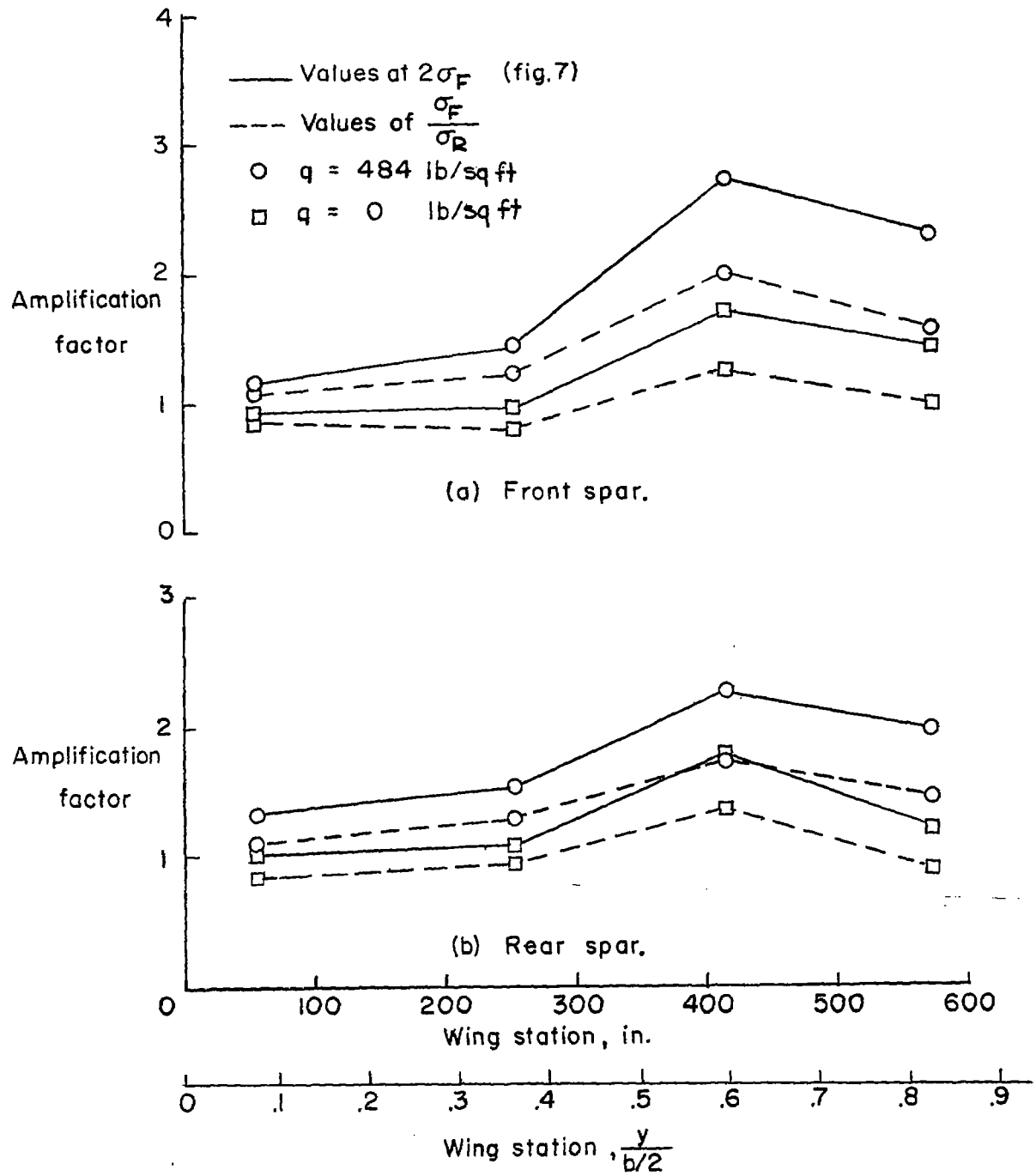

Figure 11.- Spanwise variation of amplification factor for bending strain.

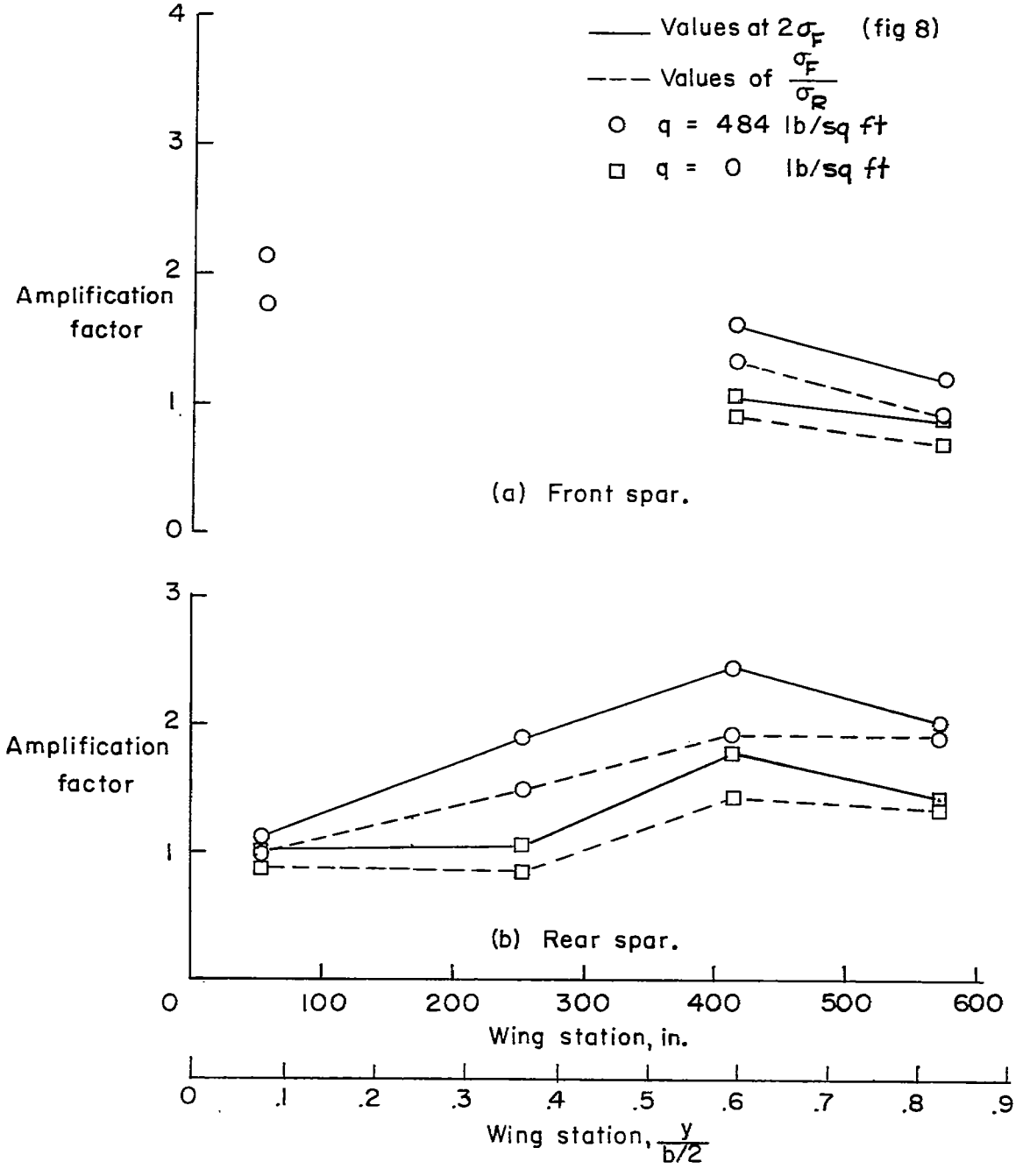

Figure 12.- Spanwise variation of amplification factor for shear strain.

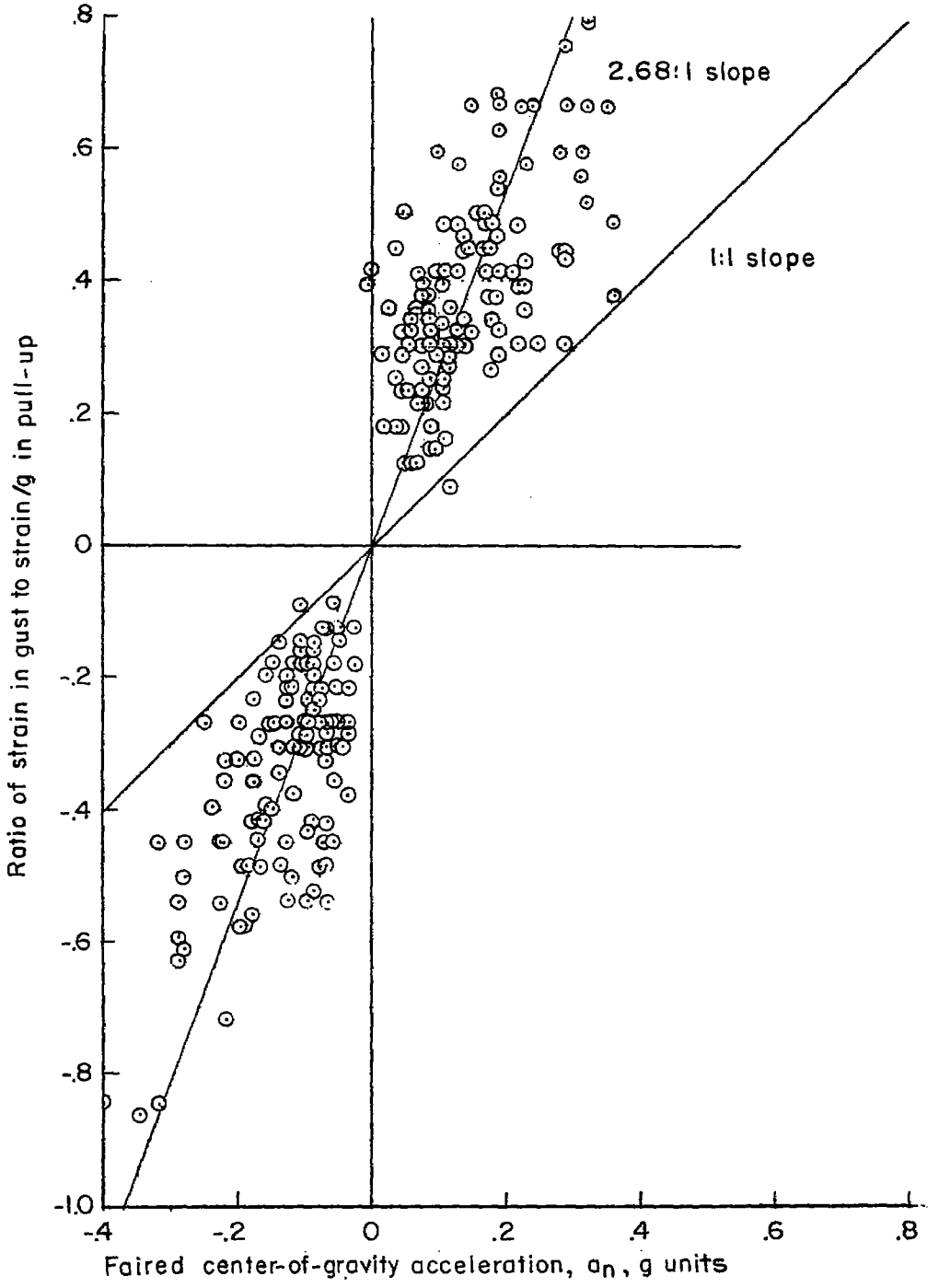

Figure 13.- Typical plot of strain ratios as a function of faired center-of-gravity acceleration. Bending-strain indication; front spar; wing station 414.